J. Fluid Mech. (2007), *vol.* 580, *pp.* 467–480.
doi:10.1017/S0022112007005617 Printed in the United Kingdom

Periodic intrusions in a stratified fluid

OLIVER S. KERR

Centre for Mathematical Science, City University, Northampton Square, London EC1V 0HB, UK

(Received 15 February 2006 and in revised form 16 January 2007)

When a salt-stratified body of fluid is heated from the side a series of almost horizontal convective layers can develop with well-mixed interiors. These layers can propagate into the interior of the stratified fluid. This behaviour is also observed with intrusions at fronts between stratified bodies of fluid where their composition varies. We look at a simplified model of intrusion growth where the mechanism behind the creation of their well-mixed interiors is neglected, and look at how a stack of such intrusions will propagate away from the wall or front. We find that there is a transition from a regime where the propagation is essentially inviscid and the intrusion length is proportional to time, to one where viscosity is important and the propagation rate slows down, with the length being proportional to the square-root of time.

1. Introduction

When a patch of fluid of uniform density is generated in an otherwise uniformly stratified fluid it undergoes collapse – it spreads out laterally at the level corresponding to its density (see De Silva & Fernando 1998, and the references therein). There are various mechanisms that could generate such a patch of fluid, for example injection of fluid of constant density from some source (Manins 1976), the localized mixing of the stratified fluid by mechanical mixing (De Silva & Fernando 1998) or breaking of internal waves. However, the basic mechanisms behind the collapsing patch of fluid and its lateral propagation are the same.

Another mechanism which gives rise to regions of almost uniform density in an otherwise stratified fluid occurs in intrusions in double-diffusive convection. For example, when a salt-stratified body of fluid experiences a horizontal temperature gradient instabilities can form that take the form of long thin almost horizontal intrusions. The source of the temperature gradient could be, for example, the heating of the salinity gradient from a sidewall (Thorpe, Hutt & Soulsby 1969; Chen, Briggs & Wirtz 1971), or the difference in properties between two bodies of fluid at a front (Ruddick & Turner 1979). In these cases a stack of intrusions is generated which have cores that may be, to a first approximation, uniform in density. Observations of intrusions in oceans and laboratories have been reviewed recently by Ruddick & Richards (2003) and Ruddick (2003) respectively. Intrusions grow away from the heated wall or front and can become very long compared to their height. They have also been observed to alter the stratification ahead of the end of the intrusions (see, for example, Schladow, Thomas & Koseff 1992; Ruddick, Phillips & Turner 1999). These have been modelled by Malki-Epshtein, Phillips & Huppert (2004) in the context of laboratory experiments where their evolution is affected by the presence of an endwall at the opposite end of the tank to the heated wall. However, we will look at the case where the flow is not affected by a distant boundary, so for the sidewall heating case

the fluid is effectively semi-infinite. This would be the case in experiments if they were conducted in sufficiently long tanks.

In order to obtain insight into the propagation of intrusions we will ignore the mechanisms which generate these intrusions at the wall or at the front between two bodies of fluid and concentrate on how they move through the stratified fluid. We will assume that the intrusions are two-dimensional and periodic, and that the diffusion of whatever is causing the density variations can be ignored. In reality the flows may be three-dimensional (Chan, Chen & Chen 2002), they may undergo some merging processes and display some variation in vertical height (Tanny & Tsinober 1989) and diffusion of density may not be negligible. In addition the cores of the cells may retain some degree of stratification (Ruddick *et al.* 1999; Malki-Epshtein *et al.* 2004). Even with our assumption of uniform density in the interior of the intrusion, our model will have some relevance to this latter case.

We will look at the large-time behaviour of the system. The small-time behaviour is associated with the mechanisms involved in the generation of the layers of constant density and so is beyond the scope of this work. We will look at the asymptotics of a model where the contribution from the viscosity terms is assumed to be dominated by the contribution from the horizontal shear. This model will show that there is an initial phase where the front of an intrusion moves away from the wall at an approximately constant speed proportional to hN, where h is the half-height of the intrusion and N is the buoyancy frequency. There is then a transition to a regime where the viscosity becomes important, and the front of an intrusion will grow at a reduced speed so that its length is proportional to $Nh^2t^{1/2}\nu^{-1/2}$ where ν is the kinematic viscosity and t the time since the intrusion first formed. In this second regime the density field ahead of the intrusion is significantly modified so that its nose is moving into a region which is almost at the density of the intrusion itself. This 'blocking' flow is generated by columnar internal waves propagating ahead of the intrusion.

There is a degree of similarity between the analysis presented here and some of that used in earlier investigations of intrusions of fluid being injected into a stratified fluid (Manins 1976), or fluid being extracted from stratified fluid (for example, Imberger 1972; Pao & Kao 1974; Imberger & Fandry 1975; Imberger, Thompson & Fandry 1976).

2. Governing equations and problem formulation

We will consider the case of a body of fluid which initially has a linear vertical density gradient. This body of fluid is bounded by a vertical wall. At some initial time some process will lead to a periodic density perturbation at the wall. This could be caused by physical mixing such as a periodic version of the experiments of De Silva & Fernando (1998) where an oscillating grid generated a patch of well-mixed fluid. Alternatively, there may be mixing caused by some other process such as heating at the wall leading to overturning convection. In both cases we will assume that the stratification in the bulk of the fluid is caused by a salinity gradient. Since salt has a diffusivity several hundred times smaller than the kinematic viscosity of water, and since we will be focusing on the case where the viscosity is, in some sense, weak we will assume that the diffusion of the salt can be neglected. The effect of temperature variations in the second example will also be ignored, but is discussed further in the concluding section.

The governing equations for the velocity, $\boldsymbol{u}=(u, v, w)$, and density perturbation, ρ, of an incompressible fluid after making the Boussinesq approximation are

$$\frac{\partial \boldsymbol{u}}{\partial t}+\boldsymbol{u}\cdot\nabla\boldsymbol{u}=-\frac{1}{\rho_0}\nabla p-\frac{g\rho}{\rho_0}\hat{\boldsymbol{z}}+\nu\nabla^2\boldsymbol{u}, \tag{2.1}$$

$$\nabla\cdot\boldsymbol{u}=0, \tag{2.2}$$

$$\frac{\partial \rho}{\partial t}+\boldsymbol{u}\cdot\nabla\rho+w\overline{\rho}_z=0, \tag{2.3}$$

where x is the horizontal coordinate measuring the distance from the wall, and z the vertical coordinate. Here ρ_0 is a reference density, $\overline{\rho}_z$ the constant vertical density gradient far from the wall, g the acceleration due to gravity and ν the kinematic viscosity. After an initial phase the disturbances will be predominantly horizontal. With variations in the vertical significantly greater than in the horizontal, and the typical horizontal velocity much greater than the typical vertical velocity we see that in the direction that the velocities are significant the density and velocity variations are small, and in the direction the density and relative velocity variations are significant the velocities are small. Hence, the advection terms in both equations can be neglected even though the velocity and variations in the density are not small (McEwan & Baines 1974). In some intrusions velocities are observed in the well-mixed core that are of the same order as those of the intrusion as a whole. Since the core is well-mixed the density will be essentially uniform and the nonlinear term in the density equation will still be negligible. In the momentum equation the effect could be to increase the effective viscosity where the flow is taken to be a mean flow. This is discussed later.

We non-dimensionalize time with respect to the inverse of the Brunt–Väisälä or buoyancy frequency, N, defined by $N^2=-g\overline{\rho}_z/\rho_0$ (Rayleigh 1883), length with respect to h, half the height of the intrusion, the velocity with respect to hN, and the density with respect to $-h\overline{\rho}_z$. Converting to a streamfunction formulation with $u=\psi_z$ and $w=-\psi_x$, we arrive at the non-dimensional equations

$$\frac{\partial\nabla^2\psi}{\partial t}=\rho_x+\epsilon\nabla^4\psi, \tag{2.4}$$

$$\frac{\partial \rho}{\partial t}+\psi_x=0, \tag{2.5}$$

where $\epsilon=\nu/(h^2N)$. All quantities in these and subsequent equations are non-dimensional. We can eliminate either the density or the streamfunction to yield a single equation for the other, for example

$$\nabla^2\rho_{tt}+\rho_{xx}-\epsilon\nabla^4\rho_t=0. \tag{2.6}$$

The boundary condition we will assume is that at the wall ($x=0$) at some initial time ($t=0$) the total density profile becomes step-like. In the region $-1<z<1$ we will assume that the total density at the wall is constant and equal to the ambient density at $z=0$ far from the wall. Hence in this region the density perturbation is given by $\rho=z$. This linear perturbation is then repeated with period 2 in the vertical. At this stage we impose no constraints on the streamfunction at the wall.

We will expand the density and streamfunction in a Fourier series in the vertical coordinate. Because the density perturbation chosen at the wall is an odd function, and we will not be forcing any of the even modes with the streamfunction boundary

conditions, we only have sine terms in these series:

$$\rho(x,z,t)=\sum_{n=1}^{\infty}\rho_n(x,t)\sin n\pi z, \qquad \psi(x,z,t)=\sum_{n=1}^{\infty}\psi_n(x,t)\sin n\pi z. \tag{2.7}$$

For other density profiles a more general Fourier series can be used in a straightforward manner. Each mode for the density series will satisfy

$$\rho_{nxxtt}-n^2\pi^2\rho_{ntt}+\rho_{nxx}-\epsilon(\rho_{nxxxxt}-2n^2\pi^2\rho_{nxxt}+n^4\pi^4\rho_{nt})=0, \tag{2.8}$$

$$\rho_n(x,0)=0, \quad x>0, \tag{2.9}$$

and for $t>0$

$$\rho_n(0,t)=\frac{2(-1)^{n+1}}{n\pi}, \quad \rho_n(x,t)\to 0 \quad \text{as} \quad x\to\infty. \tag{2.10}$$

The solution to the problem of the extraction of fluid from the midpoint of the endwall of a stratified layer can also be expressed in terms of a Fourier series similar to the above. In that case the Fourier modes of the streamfunction will satisfy a similar equation, but with different boundary conditions at the wall (Pao & Kao 1974).

We will be concerned with the case where the viscosity is weak. It would be consistent with our earlier assumptions to ignore the x-derivatives in the terms involving ∇^2 and ∇^4 in (2.6). However their neglect in the case $\epsilon=0$ would lead to the Fourier modes satisfying the one-dimensional wave equation, and so the initial jump in density at the wall would propagate to the interior without modification. In the region of the jump the x-derivatives are clearly not negligible, and so horizontal derivatives need to be retained in this region. If the ρ_{nxxtt} term from (2.8) is retained in the inviscid case then McEwan & Baines (1974) have shown that for large times it gives rise to the sharp interface being spread over a region of width proportional to $t^{1/3}$ centred on the nose of the intrusion. This behaviour is also found for the current problem when viscosity is present. We will look at the behaviour of the intrusions for large times. Having retained this ρ_{nxxtt} term from (2.8) the solutions found for the modes will be smooth for all values of x away from the wall and with ever-increasing horizontal length scales. This enables us to make the approximation that the viscous terms are dominated by the z-derivatives at all points. Our reduced system is now

$$\rho_{nxxtt}-n^2\pi^2\rho_{ntt}+\rho_{nxx}-\epsilon n^4\pi^4\rho_{nt}=0, \tag{2.11}$$

with the boundary conditions given in (2.10). With these assumptions the streamfunction modes will satisfy an equivalent equation.

Having discarded the horizontal derivatives in the viscous term we can no longer impose any additional boundary conditions at the wall beyond the density perturbation. This will give rise to solutions where ψ is not even constant at the wall, implying flow into and out of the wall at different locations (but zero net flow into the wall). This is not considered to be a problem as at the wall there will have to be some mixing process that maintains the uniform density and which will involve the entrainment and ejection of fluid from some region close to the wall. It is assumed that this process will continue, and its details will not affect the motions far from the wall at leading order.

We take Laplace transforms of (2.11), defined by

$$\hat{f}(x;s)=\int_0^{\infty} f(x,t)\,\mathrm{e}^{-st}\,\mathrm{d}t, \tag{2.12}$$

giving

$$s^2\hat{\rho}_n'' - n^2\pi^2 s^2\hat{\rho}_n + \hat{\rho}_n'' - \epsilon n^4\pi^4 s\hat{\rho}_n = 0, \tag{2.13}$$

with boundary conditions

$$\hat{\rho}_n(0;s) = \frac{2(-1)^{n+1}}{n\pi s}, \qquad \hat{\rho}_n(x;s) \to 0 \quad \text{as} \quad x \to \infty. \tag{2.14}$$

These have solutions

$$\hat{\rho}_n = \frac{2(-1)^{n+1}}{n\pi s}\exp\left[-\left(\frac{n^2\pi^2 s^2 + \epsilon n^4\pi^4 s}{1+s^2}\right)^{1/2} x\right]. \tag{2.15}$$

If an alternative density structure is maintained at the wall instead of the step-like structure assumed here, there will be different coefficients in front of the exponential terms. The Laplace transforms of the Fourier modes of the streamfunction corresponding to (2.15) are

$$\hat{\psi}_n = \frac{2(-1)^{n+1}}{n\pi}\left(\frac{1+s^2}{n^2\pi^2 s^2 + \epsilon n^4\pi^4 s}\right)^{1/2}\exp\left[-\left(\frac{n^2\pi^2 s^2 + \epsilon n^4\pi^4 s}{1+s^2}\right)^{1/2} x\right]. \tag{2.16}$$

In neither case has an exact inverse transform been found. Instead we express the solutions in terms of the inverse Laplace transform integral, for example

$$\psi_n(x,t) = \frac{1}{2\pi\mathrm{i}}\int_{\gamma-\mathrm{i}\infty}^{\gamma+\mathrm{i}\infty}\hat{\psi}_n\,\mathrm{e}^{st}\,\mathrm{d}s, \tag{2.17}$$

where γ is chosen so that the path of integration lies to the right of all the singularities of the transformed function. In both cases there are branch points at $s = \pm\mathrm{i}$, 0 and $-\epsilon n^2\pi^2$.

We will look at the large-time asymptotics of this using the method of stationary phase as used by McEwan & Baines (1974) for their investigation of shear fronts in a stratified fluid (see, for example, Hinch 1991, for more details of the method). We re-express the Fourier modes for the streamfunction as

$$\psi_n(x,t) = \frac{1}{2\pi\mathrm{i}}\int_{\gamma-\mathrm{i}\infty}^{\gamma+\mathrm{i}\infty}\frac{2(-1)^{n+1}}{n\pi}\left(\frac{1+s^2}{n^2\pi^2 s^2 + \epsilon n^4\pi^4 s}\right)^{1/2}\mathrm{e}^{f(s)t}\,\mathrm{d}s, \tag{2.18}$$

where

$$f(s) = -\left(\frac{n^2\pi^2 s^2 + \epsilon n^4\pi^4 s}{1+s^2}\right)^{1/2}\frac{x}{t} + s. \tag{2.19}$$

The large-time asymptotics are then dominated by the contribution from the saddle points of $f(s)$ which are to be found when $f'(s) = 0$. These points were determined numerically, and the local contribution to the large-time asymptotics found for each mode. The resulting asymptotic solutions could then be re-assembled to give approximations to $\psi(x,t)$ and $\rho(x,t)$.

3. Intrusion propagation

The behaviour of the growing intrusions falls into two phases for small values of ϵ. The first occurs for smaller values of t when the effects of viscosity are unimportant, and the second for larger values of t where the cumulative effect of viscosity dominates. Plots of the density perturbation, total density and streamlines for $t = 50$ and $t = 1000$ for $\epsilon = 0.001$ are shown in figures 1 and 2 respectively. The plots for $t = 50$ lie in the

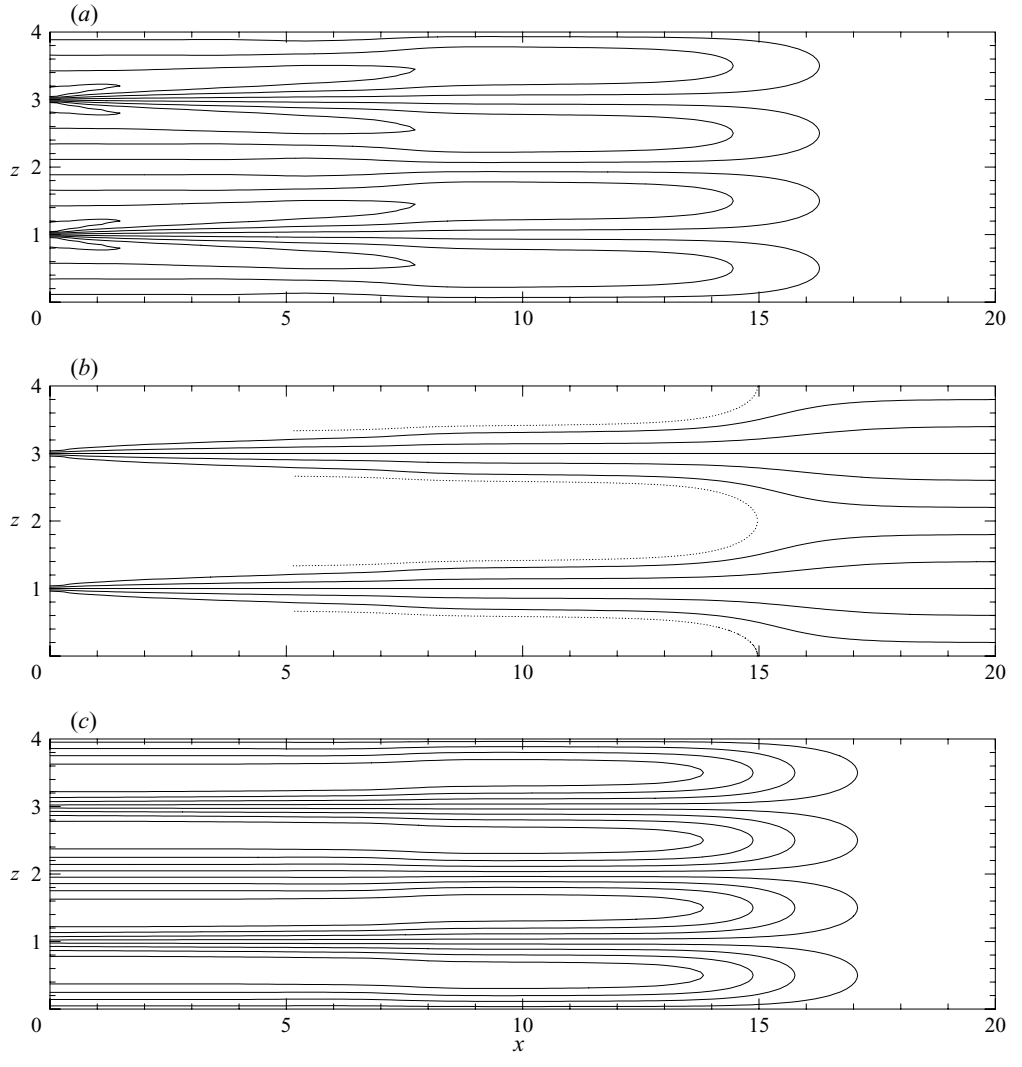

FIGURE 1. Contour plots of (*a*) density perturbation, (*b*) total density and (*c*) streamfunction for $t = 50$. The dotted line in (*b*) shows the extent of the region occupied by the intrusion consisting of fluid that has emerged from the wall. The contour intervals are (*a*) 0.25, (*b*) 0.4 and (*c*) 0.04.

first of these regimes. The individual Fourier modes propagate at speed $1/n\pi$ with an adjustment region at the front. The total density plot in figure 1(*b*) shows the position of the intrusion. This consists of fluid that has emerged from the wall since $t = 0$. It is found by following the path of fluid elements starting from near $x = 1/\pi$, $z = 0$ at $t = 1$. The flow velocity found using these asymptotics is singular for small t, and so it is not possible to integrate the velocities from $t = 0$. Since we are looking at the large-time asymptotics this is not unexpected, and the small-time behaviour of the large-time asymptotics has no particular significance. The position chosen for the initial point of the integration is approximately the position that would be found for the model in the inviscid limit. Choosing other initial values of x was found to have little effect as the frontal positions for these other values converged for larger

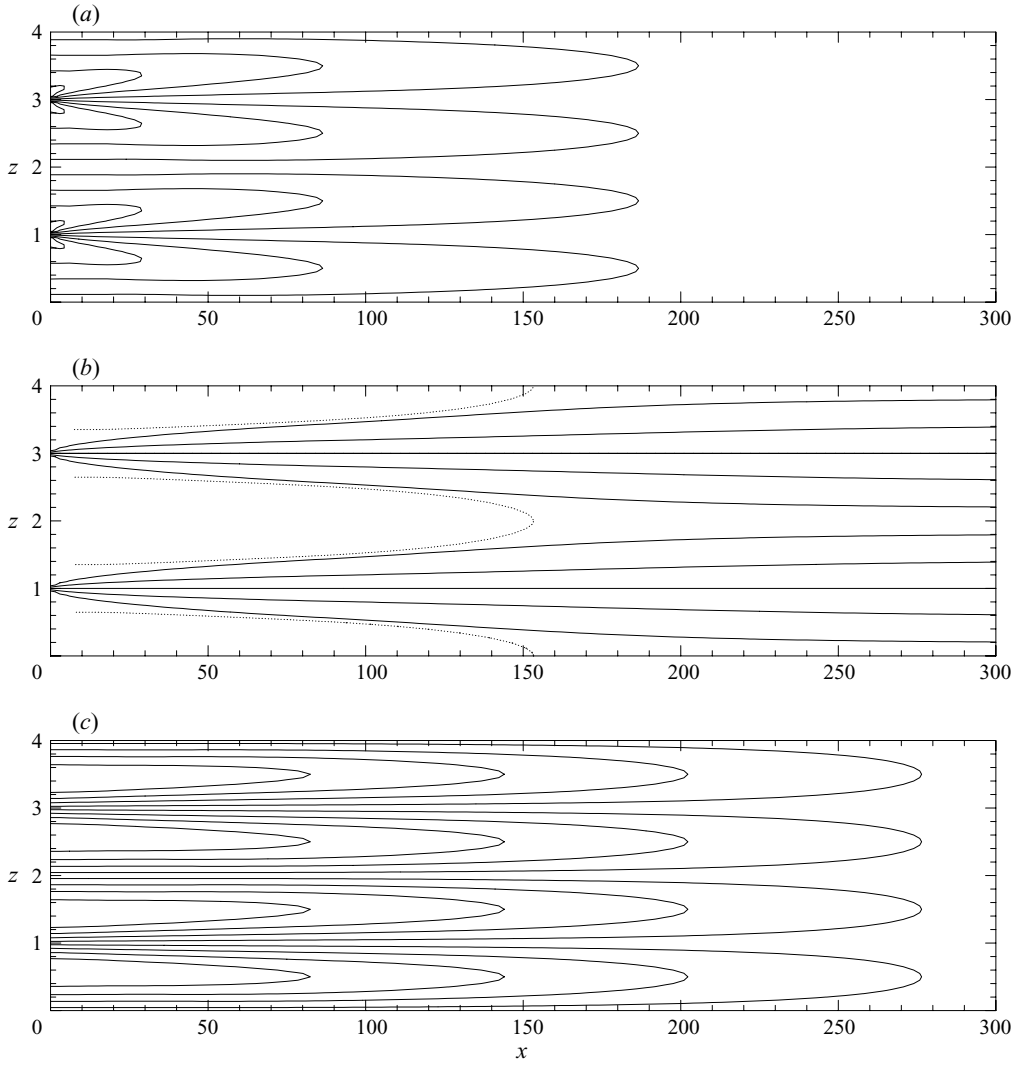

FIGURE 2. Contour plots of (*a*) density perturbation, (*b*) total density and (*c*) streamfunction for $t = 1000$. The dotted line in (*b*) shows the extent of the region occupied by the intrusion consisting of fluid that has emerged from the wall. The contour intervals are (*a*) 0.25, (*b*) 0.4 and (*c*) 0.01.

t. This is encouraging as the initial behaviour of the flow at the wall that gives rise to the mixing for a real flow will have a significant effect on the behaviour of the fluid near the wall, and in particular for small times, but we expect that for larger times the initial details of the flow will be unimportant for the overall evolution. The intrusion of the fluid emanating from the wall is relatively uniform in width. There is a relatively narrow region ahead of the intrusion where the total density adjusts to the linear density gradient to be found ahead of the nose of the intrusion.

The plots in figure 2 show the density and streamfunctions for $t = 1000$ and $\epsilon = 0.001$. This is in the second regime when the flow is significantly affected by the viscosity. The density perturbation and streamline plots show that the flow decays steadily away from the wall. The position of the intrusion in the total density plot

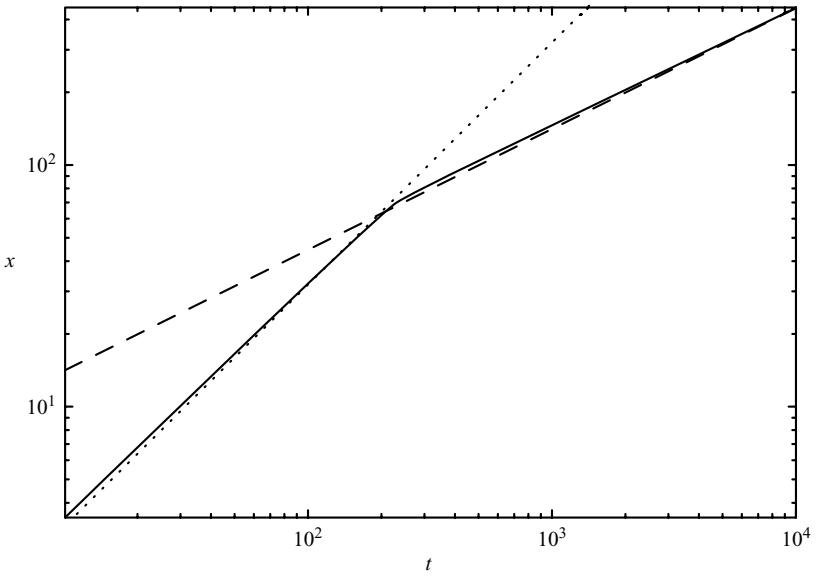

FIGURE 3. The position of the fronts of the intrusions as a function of time (————) for $\epsilon = 0.001$. Also shown are the position of the front of the intrusion in the inviscid limit (·····) and the position assuming viscosity is important (— — —).

shows that the density modification and the fluid flow extend much further ahead of the intrusion nose than in the previous case.

The variation of the position of the intrusion nose in figure 3 shows clearly the two regimes. The first part has slope approximately one in this log–log plot, indicating that the position is proportional to time. The second regime has an approximate slope of a half, indicating the front position varies roughly as $t^{1/2}$. In this regime viscosity plays a dominant role. Also indicated on this graph are asymptotic predictions for the nose position for these two regimes. The first of these is based on the inviscid model where the front of the fundamental mode propagates with velocity $1/\pi$. The second comes from the analysis of the viscous-dominated regime to be found in the following section.

4. Viscosity-dominated regime

It is found that after the transition to the second regime where viscosity is important, the disturbances ahead of the intrusions decay rapidly. The effect of the ρ_{nxxtt} term from (2.8) is only significant near the front at $x = t/(n\pi)$, where the disturbances are now very small. At all other points behind this front its effect is not significant at leading order and so away from this frontal adjustment region we can ignore this term, giving

$$n^2\pi^2\rho_{ntt} - \rho_{nxx} + \epsilon n^4\pi^4\rho_{nt} = 0. \tag{4.1}$$

The Laplace transform of the solution to this is

$$\hat{\rho}_n(x;s) = \frac{2(-1)^{n+1}}{n\pi s}\exp\left[-(n^2\pi^2s^2 + \epsilon n^4\pi^4 s)^{1/2}x\right]. \tag{4.2}$$

The equivalent solution for the Laplace transform of the streamfunction Fourier mode is

$$\hat{\psi}_n(x;s) = \frac{2(-1)^{n+1}}{n\pi(n^2\pi^2s^2 + \epsilon n^4\pi^4 s)^{1/2}} \exp\left[-(n^2\pi^2s^2 + \epsilon n^4\pi^4 s)^{1/2}x\right]. \tag{4.3}$$

For both the density and the streamfunction the singularities of the transforms consist of branch points at $s=0$ and $s=-\epsilon n^2\pi^2$. A branch cut along the real axis between these two points will ensure the transforms are analytic on the rest of the complex plane. For $n\pi x > t$ the inversion integral can be evaluated by closing the curve in the right half-plane. Since there are no singularities in this region the integral, and hence both $\psi_n(x,t)$ and $\rho_n(x,t)$, will be identically zero. The form of the viscous dissipation and the neglect of the ρ_{nxxt} term in this model does not allow information to travel ahead of the front.

If we look at the streamfunction for $n\pi x < t$ then the contour can be closed in the left half-plane, and then by deformation of this contour and change of variable the integral can be converted to

$$\psi_n(x,t) = \int_0^{\epsilon n^2\pi^2} \frac{2(-1)^{n+1}\cos\left[(\epsilon n^4\pi^4\eta - n^2\pi^2\eta^2)^{1/2}x\right]}{n\pi^2(\epsilon n^4\pi^4\eta - n^2\pi^2\eta^2)^{1/2}}\,\mathrm{e}^{-t\eta}\,\mathrm{d}\eta. \tag{4.4}$$

For large values of t this integral is dominated by the contribution near $\eta=0$. If we can ignore the quadratic terms in η in the square-root terms, then this becomes

$$\begin{aligned}\psi_n(x,t) &\approx \int_0^{\epsilon n^2\pi^2} \frac{2(-1)^{n+1}\cos\left[\epsilon^{1/2}n^2\pi^2\eta^{1/2}x\right]}{\epsilon^{1/2}n^3\pi^4\eta^{1/2}}\,\mathrm{e}^{-t\eta}\,\mathrm{d}\eta \\ &\approx \int_0^{\infty} \frac{2(-1)^{n+1}\cos\left[\epsilon^{1/2}n^2\pi^2\eta^{1/2}x\right]}{\epsilon^{1/2}n^3\pi^4\eta^{1/2}}\,\mathrm{e}^{-t\eta}\,\mathrm{d}\eta \\ &= \frac{2(-1)^{n+1}}{\epsilon^{1/2}n^3\pi^{7/2}t^{1/2}}\exp\left(-\frac{\epsilon n^4\pi^4x^2}{4t}\right),\end{aligned} \tag{4.5}$$

for sufficiently large t. Similarly we find

$$\rho_n(x,t) \approx \frac{2(-1)^{n+1}}{n\pi}\,\mathrm{erfc}\left(\frac{\epsilon^{1/2}n^2\pi^2x}{2t^{1/2}}\right), \tag{4.6}$$

where erfc is the complementary error function (see Abramowitz & Stegun 1964). This is the solution found for the simplified pair of equations

$$0 = \rho_{n_x} + \epsilon n^4\pi^4\psi_n, \qquad \rho_{n_t} + \psi_{n_x} = 0, \tag{4.7}$$

with the same boundary conditions.

Along the intrusion the maximum velocity of the fluid is found at $z=0$, where

$$u = \frac{\partial}{\partial z}\sum_{n=1}^{\infty}\psi_n(x,t)\sin n\pi z\bigg|_{z=0} = \sum_{n=1}^{\infty}\frac{2(-1)^{n+1}}{\epsilon^{1/2}n^2\pi^{5/2}t^{1/2}}\exp\left(-\frac{\epsilon n^4\pi^4x^2}{4t}\right). \tag{4.8}$$

The position of the front of the intrusion will satisfy

$$\frac{\mathrm{d}x}{\mathrm{d}t} = u(x,t), \tag{4.9}$$

and has a solution of the form $x = A(t/\epsilon)^{1/2}$, where A satisfies

$$A = \sum_{n=1}^{\infty} \frac{4(-1)^{n+1}}{n^2\pi^{5/2}} \exp\left(-\frac{n^4\pi^4A^2}{4}\right). \tag{4.10}$$

This can be solved numerically, giving $A = 0.14094$, and so the length of the viscosity-dominated intrusions, L, is given by

$$L = 0.14094(t/\epsilon)^{1/2}. \tag{4.11}$$

The comparison of this with the frontal position derived from the full problem is shown in figure 3. The nose position slightly overshoots this prediction before converging to the asymptotic solution. A simple estimate for the point of transition between the two modes can be made by finding the intersection of the two straight lines in this figure. This occurs when $t = 0.19605/\epsilon$ and $x = 0.062405/\epsilon$.

Further potentially useful information can be extracted from this solution. One method used frequently in experiments to visualize the propagation of disturbances ahead of the intrusions is to introduce a vertical line of some dye or tracer ahead of their noses. This can be done by, say, dropping potassium permanganate crystals through the stratified fluid (see, for example, Tanny & Tsinober 1988, figure 18). The vertical marker line is then distorted by the effects of the intrusions. We will look at the distortion of a line of some tracer in the fluid using the large-time asymptotic solution. We will make a couple of inappropriate assumptions in our analysis which will enable us to derive an approximate result that can then be applied to experiments where these assumptions do not apply. The first of these assumptions is that the tracer line is introduced at $t = 0$ and the second is that the displacement of the line is not too great. The second assumption allows us to look at the displacement caused by the flow at the line of insertion as if it were uniform in x. Since this assumes the lateral displacements are relatively small, we will also assume that we can ignore the vertical displacement of parts of the marker line. If we define the displacement of the line to be $\Delta X(z, t)$ from its initial position at $x = x_0$ ahead of the intrusions then it will be governed by

$$\frac{\partial \Delta X}{\partial t} = u(x_0, z, t). \tag{4.12}$$

Ahead of the intrusions $x_0 > L = A(t/\epsilon)^{1/2}$. From this we can see that the ratio of the contribution of the first mode in the Fourier expansion to the second mode is $4\exp(3\epsilon\pi^4x_0^2/(4t)) > 4\exp(3\pi^4(0.14094)^2/4) = 17.073$. In general the relative contribution from the first mode to that of the others will be greater than this, so we will look at just the effect of the first mode, i.e. taking as our model

$$\frac{\partial \Delta X}{\partial t} = \frac{2}{\epsilon^{1/2}\pi^{5/2}t^{1/2}} \exp\left(-\frac{\epsilon\pi^4x_0^2}{4t}\right) \cos \pi z. \tag{4.13}$$

Hence

$$\Delta X = \frac{2\cos \pi z}{\epsilon^{1/2}\pi^{5/2}} \left(2t^{1/2} \exp\left(-\frac{\epsilon\pi^4x_0^2}{4t}\right) - \epsilon^{1/2}\pi^{5/2}x_0 \operatorname{erfc}\left(\frac{\epsilon^{1/2}\pi^2x_0}{2t}\right)\right). \tag{4.14}$$

This can be rearranged to give

$$\Delta X/L = \left[\frac{4}{\pi^{5/2}A} \exp\left(-\frac{\pi^4A^2}{4}\left(\frac{x_0}{L}\right)^2\right) - 2\left(\frac{x_0}{L}\right) \operatorname{erfc}\left(\frac{\pi^2A}{2}\left(\frac{x_0}{L}\right)\right)\right] \cos \pi z. \tag{4.15}$$

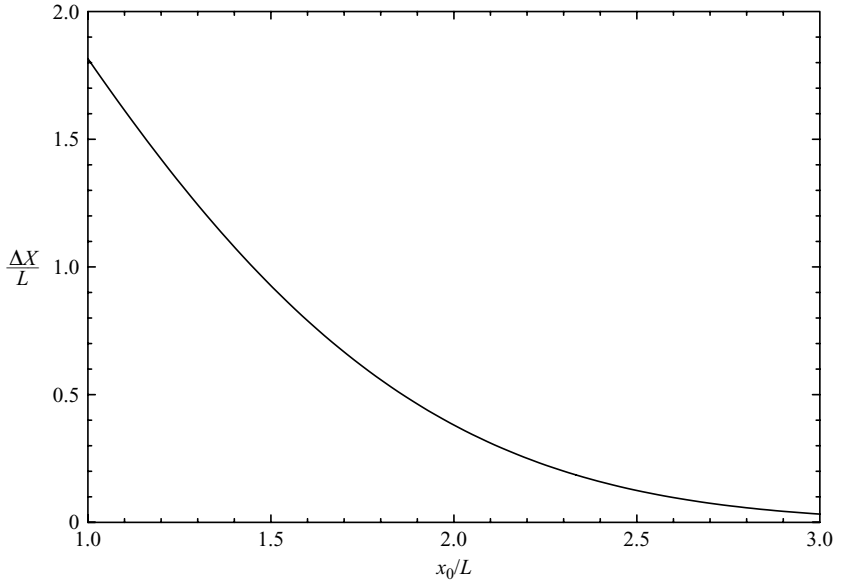

FIGURE 4. Graph of the ratio of the amplitude of the deviation of a tracer line placed at x_0 at $t = 0$ to the intrusion length, L, as a function of x_0/L.

A graph of the amplitude of $\Delta X/L$ as a function of x_0/L is shown in figure 4. From this it is clear why the original assumptions that the displacements were relatively small and that the variation of the horizontal velocity with x could be ignored are not valid for tracer lines put in place at $t = 0$ as their displacement and velocity variation would be significant for x_0/L much below $2\frac{1}{2}$. However this is not too much of a limitation in real experimental observations as the tracer lines are not usually put in place at $t = 0$ but at some later time, and observed soon afterwards when these assumptions would be valid. To find the expected amplitude of the displacement of the tracer line placed at $x = x_0$ at $t = t_0$ at some later time one just needs to find the change in the tracer line displacement predicted by the above model between t_0 and the time of the observation. If this is done then the assumptions made will indeed be appropriate. However, care must be taken to ensure that the assumptions in this model are appropriate when looking at experiments. For example, in figure 18(f) of Tanny & Tsinober (1988) three dye traces are shown ahead of double-diffusive intrusions generated by heating a salinity gradient from a sidewall. Although the magnitude of the displacement of the middle streak is in reasonable agreement with the theory, the one furthest from the wall seems to have a displacement that is too big, while the one nearest the intrusions has a displacement that is too small. In this case the intrusions had smaller heights when they first formed, and subsequently underwent a series of merging events. Accounting for these changes is beyond the scope of the theory presented here.

5. Discussion

We have looked at the propagation of well-mixed periodic intrusions into a linearly stratified body of fluid. We have identified two regimes of propagation: an almost constant-speed regime where the density perturbation propagates as inviscid internal

waves, followed by a phase where viscosity becomes important and the speed of propagation decreases as $t^{-1/2}$. This phenomenon has also been observed in single collapsing patches of fluid of uniform density by De Silva & Fernando (1998).

The speed of advancing intrusions is often compared to hN. This often yields good results as would be expected from our analysis, at least initially. For experiments where the intrusions are tracked for a longer time there is clear evidence that their advance can slow down. For example, Jeevaraj & Imberger (1991) noticed such a reduction and derived a model that predicted that the nose displacement for intrusions would be of order $t^{1/4}$. This model is based on the advection of heat in the intrusions. Although consistent with the observations of their experiments the predictions using Jeevaraj & Imberger's model were found by Malki-Epshtein *et al.* (2004) to be inconsistent with their later results.

The model of Malki-Epshtein *et al.* (2004) for intrusions in a finite tank predicted an initial stage where the intrusion speed was almost constant and scaled as hN before the effects of the far endwall came into play. However, their observations of this speed were typically smaller than $1/\pi$. This is consistent with their observation that the interior of their intrusions retained a density stratification. The precise way in which this density stratification will evolve is not clear. Some insight can be obtained by considering a reduction in the density stratification inside the intrusions, while maintaining its linear nature. The solution for this problem is just the solution found here but with all the Fourier coefficients for the density and streamfunction multiplied by a factor between zero and one. The propagation speed of the internal wave fronts is unaffected, and so the density adjustment to that at the wall occurs essentially as before. However the propagation speed of the fronts of the intrusions will be reduced, and so the region of modified density in front of the intrusions will be extended.

Both the models of Jeevaraj & Imberger (1991) and Malki-Epshtein *et al.* (2004) incorporated more complicated phenomena than considered here, where an attempt has been made to keep matters as simple as possible.

When intrusions are driven by the heating of a salinity gradient from a sidewall, there will also be temperature differences in and along the intrusions, and the associated density differences will play a role. However, owing to the relatively large diffusivity of heat compared to that of salt the temperature diffuses more rapidly and has been observed to give rise to relatively small vertical variations in temperature. A decreasing temperature is established along the intrusions which will cause the intrusions to slope downwards (or upwards if the wall is cooled). This will not significantly alter the dynamics looked at here.

Where the intrusions are caused by lateral differences in the composition of two bodies of water and not heat (for example sugar and salt differences in Ruddick & Turner 1979) the simple model presented here may not be entirely appropriate if the diffusivities of the two components are similar in magnitude, or indeed if the faster diffusing component is involved in the stratification away from the wall. Investigations into the structure of intrusions driven by salt/sugar differences have been carried out by Ruddick *et al.* (1999) and Ruddick (2003), where some of the extra complexities become apparent. In some circumstances gradients of temperature and salinity in the stratified fluid can drive active convection along the length of the intrusions, releasing further energy into the motions. In this case the dynamics will not necessarily be closely linked to what happens at the wall, and intrusions could propagate with constant speed indefinitely (Schladow *et al.* 1992).

The examples of double-diffusive intrusions cited here have fixed temperature or compositional differences across the regions of intrusions, and the average intrusion

height remains essentially constant. In other cases such as Suzukawa & Narusawa (1982) a constant heat flux was applied at the wall, and so the temperature difference across the intrusions and the average intrusion height were both continually increasing. In these cases the theory presented here will not be applicable as the density profile at the wall will be constantly changing, and the use of a Fourier series expansion would not be appropriate.

There are other difficulties associated with applying the results here to, say, oceanic intrusions. When the core of the intrusions is effectively turbulent then the effective eddy viscosity and diffusivities become comparable, at least in the core of the intrusions. If the intrusions develop relatively sharp interfaces between them with density jumps over a relatively short distance, then there may be local variations in the local effective diffusivities that will be important. Such effects have been looked at by Walsh & Ruddick (1995). Since the interfaces between the intrusions remain relatively sharp the effective eddy diffusivity in the region of significant density gradients must be relatively small, and so the model considered here may well be appropriate.

It is clear that this model does not correspond precisely to any real problem, but incorporates some of the features of other systems, such as the propagation of intrusions driven by the heating or cooling of a salinity gradient from a sidewall. These real intrusions are more complex, with additional features that have to be incorporated, such as the details of how the flow towards the wall is entrained into the intrusions, and the effect of having a finite tank (see Malki-Epshtein *et al.* 2004). However, in all cases the intrusions are propagating into a linear stratification, and the interaction between the intrusions and the ambient fluid needs to be taken into account. It is hoped that some of the ideas developed here will be incorporated into more complete models of intrusions.

The hospitality of the Department of Oceanography, Dalhousie University where much of this work was conducted, and in particular that of Barry Ruddick is gratefully acknowledged.

REFERENCES

Abramowitz, M. & Stegun, I. A. 1964 *Handbook of Mathematical Functions*. Dover.

Chan, C. L., Chen, W.-Y. & Chen, C. F. 2002 Secondary motion in convection layers generated by lateral heating of a solute gradient (with an Appendix by O. S. Kerr). *J. Fluid Mech.* **455**, 1–19.

Chen, C. F., Briggs, D. G. & Wirtz, R. A. 1971 Stability of thermal convection in a salinity gradient due to lateral heating. *Intl J. Heat Mass Transfer* **14**, 57–65.

De Silva, I. P. D. & Fernando, H. J. S. 1998 Experiminets on collapsing turbulent regions in stratified fluids. *J. Fluid Mech.* **358**, 29–60.

Hinch, E. J. 1991 *Perturbation Methods*. Cambridge University Press.

Imberger, J. 1972 Two-dimensional sink flow of a stratified fluid contained in a duct. *J. Fluid Mech.* **53**, 329–349.

Imberger, J. & Fandry, C. 1975 Withdrawal of a stratified fluid from a vertical two-dimensional duct. *J. Fluid Mech.* **70**, 321–332.

Imberger, J., Thompson, R. & Fandry, C. 1976 Selective withdrawal from a finite rectangular tank. *J. Fluid Mech.* **78**, 489–512.

Jeevaraj, C. G. & Imberger, J. 1991 Experimental study of double-diffusive instability in sidewall heating. *J. Fluid Mech.* **222**, 565–586.

Malki-Epshtein, L., Phillips, O. M. & Huppert, H. E. 2004 The growth and structure of double-diffusive cells adjacent to a cooled side-wall in a salt-stratified environment. *J. Fluid Mech.* **518**, 347–362.

Manins, P. C. 1976 Intrusions into a stratified fluid. *J. Fluid Mech.* **74**, 547–560.

McEwan, A. D. & Baines, P. G. 1974 Shear fronts and and experimental stratified shear flow. *J. Fluid Mech.* **63**, 257–272.

Pao, H.-S. & Kao, T. W. 1974 Dynamics of establishment of selective withdrawal of a stratified fluid from a line sink. Part 1. Theory. *J. Fluid Mech.* **65**, 657–688.

Rayleigh, Lord 1883 Investigation of the character of the equilibrium of an incompressible heavy fluid of variable density. *Proc. Lond. Math. Soc.* **14**, 170–177.

Ruddick, B. R. 2003 Laboratory studies of interleaving. *Prog. Oceanogr.* **56**, 529–547.

Ruddick, B. R., Phillips, O. M. & Turner, J. S. 1999 A laboratory and quantitative model of finite-amplitutde thermohaline intrusions. *Dyn. Atmos. Oceans* **30**, 71–99.

Ruddick, B. R. & Richards, K. 2003 Oceanic thermohaline intrusions: observations. *Prog. Oceanogr.* **56**, 499–527.

Ruddick, B. R. & Turner, J. S. 1979 The vertical length scale of double-diffusive intrusions. *Deep-Sea Res.* **26**, 903–913.

Schladow, S. G., Thomas, E. & Koseff, J. R. 1992 The dynamics of intrusions into a thermohaline stratification. *J. Fluid Mech.* **236**, 127–165.

Suzukawa, Y. & Narusawa, U. 1982 Structure of growing double-diffusive convection cells. *Trans. ASME: J. Heat Transfer* **104**, 248–254.

Tanny, J. & Tsinober, A. B. 1988 The dynamics and structure of double-diffusive layers in sidewall-heating experiments. *J. Fluid Mech.* **196**, 135–156.

Tanny, J. & Tsinober, A. B. 1989 On the behaviour of a system of double diffusive layers during its evolution. *Phys. Fluids* A **1**, 606–609.

Thorpe, S. A., Hutt, P. K. & Soulsby, R. 1969 The effects of horizontal gradients on thermohaline convection. *J. Fluid Mech.* **38**, 375–400.

Walsh, D. & Ruddick, B. 1995 Double-diffusive interleaving: the influence of non-constant diffusivities. *J. Phys. Oceanogr.* **25**, 348–358.